ARTICLES

Competition between Intramolecular Electron-Transfer and Energy-Transfer Processes in Photoexcited Azulene−C_{60} Dyad

Takashi Makinoshima,[†] Mamoru Fujitsuka,[†,‡] Mikio Sasaki,[†] Yasuyuki Araki,[†] Osamu Ito,*[,†] Shunji Ito,[§,||] and Noboru Morita[§]

Institute of Multidisciplinary Research for Advanced Materials, Tohoku University, Katahira, Aoba-ku, Sendai 980-8577, Japan, and Department of Chemistry, Graduate School of Science, Tohoku University, Aramaki Aza Aoba, Aoba-ku, Sendai 980-8578, Japan

Received: January 29, 2003; In Final Form: November 11, 2003

Photoinduced intramolecular processes in a dyad of azulene and C_{60} (Az−C_{60}) were compared with those of a dyad of naphthalene and C_{60} (Naph−C_{60}) on the basis of laser flash photolysis experiments. Upon photoexcitation of C_{60} in the presence of azulene, intermolecular electron transfer proceeded from azulene to the triplet state of C_{60} ($C_{60}(T_1)$), although the rate constant was small (10^7 M^{-1} s^{-1}), because of the small free-energy change for electron transfer via $C_{60}(T_1)$. In Az−C_{60}, it was revealed that the S_2 state of the Az moiety ($Az(S_2)$−$C_{60}(S_0)$) donates the excited energy to the C_{60} moiety, effectively generating $Az(S_0)$−$C_{60}(S_1)$. In polar solvents, a charge-separated state ($Az^{\bullet+}$−$C_{60}^{\bullet-}$) was generated from $Az(S_0)$−$C_{60}(S_1)$, from which the S_1 state of the Az moiety ($Az(S_1)$−$C_{60}(S_0)$) was also generated by competitive energy transfer. The lifetimes of the charge-separated states were on the order of nanoseconds. Successive energy-transfer processes {$Az(S_2)$−$C_{60}(S_0) \rightarrow Az(S_0)$−$C_{60}(S_n)$, $Az(S_0)$−$C_{60}(S_1) \rightarrow Az(S_1)$ −$C_{60}(S_0)$, where $n \geq 2$} demonstrate that the multiple energy transfer is achieved in a simple dyad molecule. On the other hand, Naph−C_{60} dyad did not show charge separation upon excitation of the C_{60} moiety, but deactivated via intersystem crossing, generating almost quantitatively the $C_{60}(T_1)$ moiety. These findings indicate the favorable donor ability of azulene compared to that of naphthalene, even though both azulene and naphthalene have the same 10-π-electron system.

Introduction

Studies on dyad systems containing redox-active and photoactive chromophores are valuable for designing light-energy-harvesting systems as well as for developing molecular devices such as optoelectronic devices.[1] Many researchers have attempted to optimize the charge-separation processes by mimicking the natural photosynthesis systems including reaction centers and antenna groups, in which highly efficient and long-lived charge separation and multiple-step energy transfer have been attained.[1] Recently, fullerenes have been employed as electron acceptors of the dyad compounds owing to their three-dimensional structure, reduction potentials comparable to those of benzoquinones, absorption spectra covering most of the visible region, and a small reorganization energy for electron-transfer reactions.[2−10] For the donor of the dyads, various compounds such as aromatic amino compounds,[2] carotenoids,[3] porphyrins,[4] tetrathiafulvalenes,[5] oligothiophenes,[6] and so on[7−10] have been employed. For these dyad molecules including fullerene, fast charge separation and long-lived charge-separated states have been reported.[2−10]

Azulene has a 10-π-electron system as does naphthalene. However, the properties of azulene in the ground and excited states are quite different from those of naphthalene. Azulene is an electron donor, and has the absorption band in the visible region. These properties are attributed to the small HOMO−LUMO gap of azulene.[11] Furthermore, azulene is one of the molecules exhibiting S_2−S_0 fluorescence. It has been reported that the S_1 state decays to the ground state within 1 ps by a nonradiative pathway.[12] It is interesting to investigate the photoinduced processes, to which the S_2 state of azulene contributes. Recently, Yeow and Steer reported intramolecular energy transfer from the S_2 state of azulene to the S_2 state of zinc porphyrin.[13]

In the presence of an electron acceptor such as fullerene, C_{60}, contributions of the S_1 and S_2 states of azulene to the photoinduced intramolecular and intermolecular processes will be elucidated. In the present study, we have studied the photoinduced processes of a dyad molecule including azulene and C_{60} (Az−C_{60}; Chart 1) by primarily using laser flash photolysis. Intramolecular charge-separation and energy-transfer processes in Az−C_{60} dyad were investigated as a function of solvent polarity. These results were compared with a naphthalene−C_{60} dyad (Naph−C_{60}; Chart 1), which has a donor moiety with the same 10-π-electron system. Furthermore, a multiple-energy-transfer process was observed in the present dyad. In addition, the intermolecular processes between C_{60} and azulene were compared with the intramolecular processes of Az−C_{60} dyad.

[†] Institute of Multidisciplinary Research for Advanced Materials, Tohoku University.

[‡] Present address: The Institute of Scientific and Industrial Research, Osaka University, Osaka 567-0047, Japan.

[§] Graduate School of Science, Tohoku University.

[||] Present address: Department of Materials Science, Hirosaki University, Hirosaki 036-8651, Japan.

10.1021/jp0342428 CCC: $27.50
Published on Web 12/20/2003

CHART 1

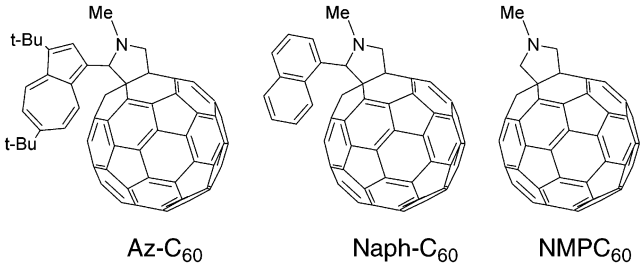

Experimental Section

Materials. Buckminsterfullerene, C_{60} (+99.95%), was obtained from Terms Co. 1,6-Di-*tert*-butylazulene (BuAz) was synthesized according to the procedure reported previously.[14] Other chemicals and solvents used in the present study were all the purest grade commercially available. Az−C_{60} was synthesized from 3,6-di-*tert*-butylazulene-1-carbaldehyde[14] by the Prato method:[15] The mixture of *N*-methylglycine (49.8 mg, 0.42 mmol), 3,6-di-*tert*-butylazulene-1-carbaldehyde (5.2 mg, 0.028 mmol), and C_{60} (30 mg, 0.042 mmol) in toluene (40 mL) was refluxed for 15 h under a nitrogen atmosphere. Then, solvent was evaporated, and the residue was purified by the column chromatography (silica gel, toluene:hexane = 1:1). After recrystallization using a hexane−methanol mixture, brown solid (7.4 mg, 26.4%) was obtained. Spectroscopic data: ^{1}H NMR (400 MHz, C_6D_6) δ/ppm 1.21 (s, 9H), 1.58 (s, 9H), 2.61 (s, 3H), 4.26 (s, 1H), 4.64 (d, J = 9.3 Hz, 2H), 6.97 (d, J = 7.3 Hz, 1H), 7.01 (d, J = 7.3 Hz, 1H), 7.12 (d, J = 10.5 Hz, 1H), 7.13 (s, 1H), 8.49 (d, J = 10.5 Hz, 1H); MALDI-TOF-MS *m*/*z* found 1005.73 (M^+ (calcd 1005.04) or $M^+ + H^+$ (calcd 1006.05)). Naph−C_{60} was synthesized in the same manner from C_{60} and naphthalene-1-carbaldehyde. *N*-Methylpyrrolidino-C_{60} (NMPC_{60}; Chart 1) was synthesized according to the reported procedure.[16]

Apparatus. The subpicosecond transient absorption spectra were observed by the pump and probe method. The samples were excited with the laser light (second harmonic generation (SHG), 388 nm) from a femtosecond Ti:sapphire regenerative amplifier seeded by SHG of an Er-doped fiber laser (Clark-MXR CPA-2001 plus, 1 kHz, fwhm 150 fs). The excitation light was depolarized. A white continuum pulse generated by focusing the fundamental light on a H_2O cell was used as a monitoring light. The visible monitoring light transmitted through the sample was detected with a dual MOS detector (Hamamatsu Photonics, C6140) equipped with a polychromator (Acton Research, SpectraPro 150). For detection of the near-IR light, an InGaAs linear image sensor (Hamamatsu Photonics, C5890-128) was employed. The spectra were obtained by averaging on a microcomputer.[6f]

Nanosecond transient absorption measurements were carried out using the laser light (SHG, 532 nm) of a Nd:YAG laser (fwhm 6 ns) as an excitation source. The probe light from a pulsed Xe lamp was detected with a Ge-avalanche photodiode equipped with a monochromator after passing through the sample in a quartz cell (1 cm × 1 cm). Phenomena on a long time scale were observed using a photomultiplier tube as a detector. Sample solutions were deaerated by bubbling Ar gas through the solutions for 15 min. Details of the transient absorption measurements were described in our previous papers.[6b,c,f]

Fluorescence lifetimes were measured by a single-photon-counting method using a streakscope (Hamamatsu Photonics, C4334-01). The samples were excited with the laser light (SHG, 410 nm) of a Ti:sapphire laser (Spectra-Physics, Tsunami 3950-L2S, fwhm 1.5 ps) pumped by an argon ion laser (Spectra-Physics, BeamLok 2060-10-SA). Steady-state fluorescence spectra of the samples were measured on a Shimadzu RF-5300PC spectrofluorophotometer.

Steady-state absorption spectra in the visible and near-IR regions were measured on a Jasco V530 spectrophotometer.

Cyclic voltammetry measurements were carried out using a BAS CV50W voltammetric analyzer in a conventional three-electrode cell employing Pt working and counter electrodes and an Ag/Ag^+ reference electrode at a 100 mV s^{-1} of scan rate. Sample solutions containing 0.1 M tetrabutylammonium perchlorate were deaerated by Ar-bubbling before measurements.

Molecular Orbital Calculations. All calculations were made using the Gaussian 98 package.[17] Geometry optimization and calculations of molecular orbital coefficients were performed at the ab initio B3LYP/6-31G* level.

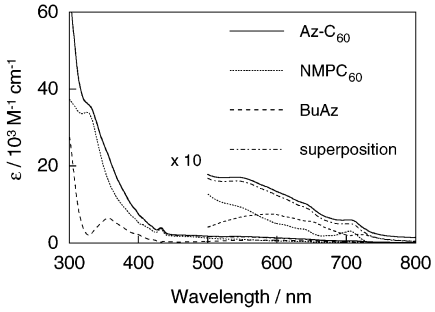

Figure 1. Steady-state absorption spectra of Az−C_{60}, NMPC_{60}, and BuAz and a superposition of the spectra of NMPC_{60} and BuAz in toluene.

TABLE 1: Oxidation and Reduction Potentials of Az−C_{60}, Naph−C_{60}, NMPC_{60}, and BuAz in Benzonitrile

compound	$E(C_{60}^{\bullet-}/C_{60})^a$	$E(D/D^{\bullet+})^{a,b}$	$E(C_{60}/C_{60}^{\bullet+})^a$
Az−C_{60}	−0.90	0.65	[c]
Naph−C_{60}	−0.88	1.19	0.76
NMPC_{60}	−0.88		0.76
BuAz		0.70	

[a] Potential vs Ag/Ag^+. [b] D = Az, Naph, and BuAz. [c] Difficult to estimate due to overlap with $E(D/D^{\bullet+})$.

Results and Discussion

Steady-State Spectra of the Dyads. Steady-state absorption spectra of Az−C_{60} dyad, BuAz, and NMPC_{60} in toluene are shown in Figure 1. The absorption spectrum of Az−C_{60} dyad does not show a significant change within the experimental error compared to the superposition of the spectra of BuAz and NMPC_{60}. This finding indicates the absence of significant interaction between the Az and C_{60} moieties in the ground state.

In the present study, laser excitation of Az−C_{60} dyad was carried out using the 388 or 355 nm laser light. At 388 and 355 nm, the C_{60} and Az moieties absorbed the laser light at a ratio of 72:28.

Cyclic Voltammetry. In the cyclic voltammogram, Az−C_{60} dyad showed oxidative and reductive waves at 0.65 and −0.90 V vs Ag/Ag^+, which are assigned to $E(Az/Az^{\bullet+})$ and $E(C_{60}^{\bullet-}/C_{60})$, respectively, by comparison to the corresponding model compounds (Table 1). These oxidation and reduction potentials are essentially the same as those of the model compounds, suggesting a small interaction between the Az and C_{60} moieties as indicated by the steady-state absorption spectra. In the case of Naph−C_{60} dyad, two oxidative waves were confirmed at 0.76 and 1.19 V vs Ag/Ag^+, due to $E(C_{60}/C_{60}^{\bullet+})$ and $E(Naph/Naph^{\bullet+})$, respectively, in addition to the reductive wave at −0.88

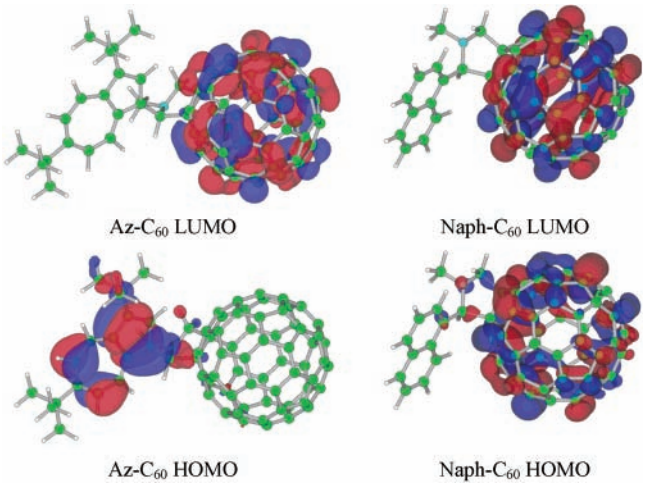

Figure 2. HOMOs and LUMOs of Az−C_{60} and Naph−C_{60} calculated at the B3LYP/6-31G* level.

V vs Ag/Ag^+, due to $E(C_{60}^{\bullet-}/C_{60})$. This finding indicates that the Naph moiety of Naph−C_{60} dyad has lower electron-donor ability than the Az moiety of Az−C_{60} dyad.

MOs of the Dyads. Optimized structures and MOs were estimated at the B3LYP/6-31G* level. In the case of Az−C_{60} dyad, the HOMO is on the Az moiety, while the LUMO is delocalized on the C_{60} moiety as shown in Figure 2. This fact accords with the result of cyclic voltammetry, in which the first oxidative wave was assigned to the Az moiety of the dyad and the first reductive wave to the C_{60} moiety. Thus, the absorption band due to the charge-transfer complex is anticipated to appear at longer wavelength than 705 nm as the lowest transition, although the absorption was too weak to observe. This finding indicates that charge separation was possible upon the excitation of Az−C_{60} dyad.

For Naph−C_{60} dyad, on the other hand, both the HOMO and LUMO are on the C_{60} moiety of the dyad. Contribution of the Naph moiety was confirmed in the HOMO−1. These findings are also in accord with the cyclic voltammogram, in which the first oxidative and reductive waves were assigned to the C_{60} moiety, while the second oxidation was attributed to E(Naph/$Naph^{\bullet+}$). Thus, the contribution of the Naph moiety of Naph−C_{60} dyad to the lowest excited state will be small in contrast to that of Az−C_{60} dyad.

Photoinduced Intermolecular Electron Transfer from Azulene to C_{60}. At first, photoinduced intermolecular processes of C_{60} in the presence of BuAz were investigated to confirm the donor ability of azulene to the excited state of C_{60}. In the presence of BuAz in benzonitrile, transient absorption spectra observed by the excitation of C_{60} with the 355 nm laser are shown in Figure 3, in which the transient absorption band appeared at 740 nm immediately after the laser irradiation. The 740 nm band was attributed to the triplet state of C_{60} ($C_{60}(T_1)$). With the decay of $C_{60}(T_1)$, an absorption band of the radical anion of C_{60} ($C_{60}^{\bullet-}$) appeared at 1080 nm. In the spectrum observed at 10 μs after the laser pulse, the absorption band remained in the 400−800 nm region, which can be attributed to the overlap of absorption of $BuAz^{\bullet+}$ with that of $C_{60}^{\bullet-}$ in this visible region, where both radical ions have the absorption band. Since $C_{60}^{\bullet-}$ does not exhibit a substantial absorption band in the 600−800 nm region, the band around 780 nm may be due to $BuAz^{\bullet+}$ mainly as well as the peak around 550 nm. Anyway, the absorptions of $BuAz^{\bullet+}$ are expected to be small compared with that of $C_{60}^{\bullet-}$ at 1080 nm, because of a quite small extinction coefficient of $BuAz^{\bullet+}$ (<300 M^{-1} cm^{-1} for

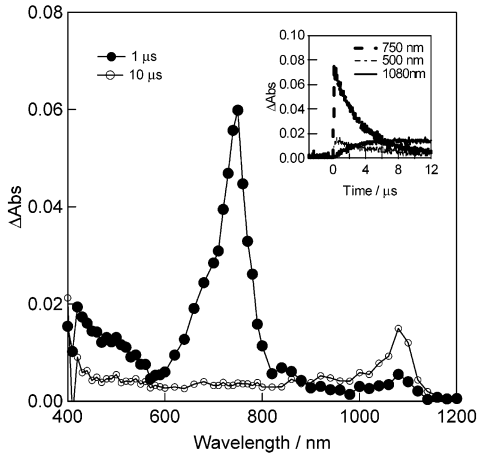

Figure 3. Transient absorption spectra observed by 532 nm laser light excitation of C_{60} (0.1 mM) in the presence of BuAz (1 mM) in deaerated benzonitrile. Inset: absorption−time profiles.

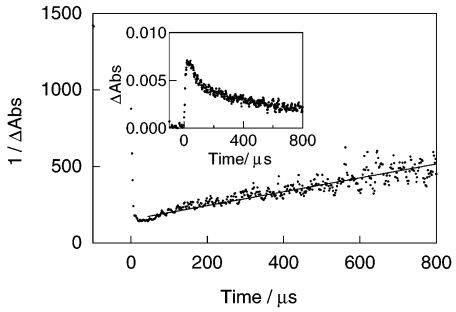

Figure 4. Second-order plot for decay of the radical anion of C_{60} at 1080 nm in deaerated benzonitrile. Inset: absorption−time profile.

the peak around 800 nm)[18,19] compared to that of $C_{60}^{\bullet-}$ (16100 M^{-1} cm^{-1} at 1080 nm).[20] These findings support that intermolecular electron transfer proceeded from BuAz to $C_{60}(T_1)$ as shown in eq 1, where k_{et}^T is a rate constant for the electron-transfer process.

$$C_{60}(T_1) + BuAz \xrightarrow{k_{et}^T} C_{60}^{\bullet-} + BuAz^{\bullet+} \qquad (1)$$

The decay rate of $C_{60}(T_1)$ and the rise rate of $C_{60}^{\bullet-}$ increased with an increase in the concentration of BuAz. From the pseudo-first-order plot, the triplet quenching rate constant (k_q^T) was estimated to be 1.0×10^8 M^{-1} s^{-1}. The quantum yield (Φ_{et}^T) for the intermolecular electron transfer via $C_{60}(T_1)$ can be calculated from the ratio of the maximal concentration of $C_{60}^{\bullet-}$ to the initial concentration of $C_{60}(T_1)$. The Φ_{et}^T value was evaluated to be 0.6 for the present mixture system. Thus, the k_{et}^T value was calculated to be 6.0×10^7 M^{-1} s^{-1} from the relation $k_{et}^T = \Phi_{et}^T k_q^T$.[21] The estimated k_q^T and k_{et}^T values are quite small compared to the diffusion-limiting rate of the solvent ($k_{diff} = 5.3 \times 10^9$ M^{-1} s^{-1} in benzonitrile).[22] The small k_q^T, Φ_{et}^T, and k_{et}^T values are in accord with a prediction based on the free-energy change for the intermolecular electron-transfer process (ΔG_{et}^T), which was calculated to be −0.02 eV.[23] These findings indicate that BuAz is a weak donor to $C_{60}(T_1)$. In the case of a mixture system of C_{60} and naphthalene, no electron transfer was observed even when the concentration of naphthalene was increased, indicating that naphthalene does not work as an electron donor to $C_{60}(T_1)$.

The absorption intensity of $C_{60}^{\bullet-}$ at 1080 nm decayed slowly after reaching a maximum (inset of Figure 4). This decay obeyed second-order kinetics and was attributed to the back-electron-transfer process because any evidence for other reaction

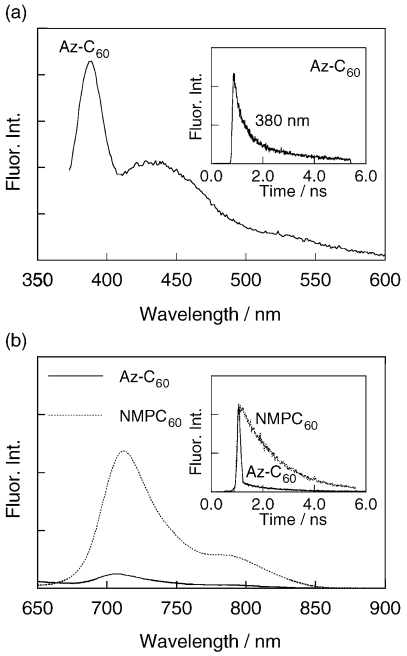

Figure 5. (a) Fluorescence spectrum of Az−C_{60} (excitation 345 nm) in the 350−600 nm region and (b) Az−C_{60} and $NMPC_{60}$ (excitation 380 nm) in the 650−900 nm region in toluene. Inset: fluorescence decay profiles of Az−C_{60} and $NMPC_{60}$.

processes was not confirmed from the steady-state absorption of the solution after laser irradiation. From the slope of the second-order plot, a rate constant for the back electron transfer (k_{bet}) was evaluated to be 4.2×10^9 M^{-1} s^{-1}. The k_{bet} value is almost the same as the k_{diff} value, because of a sufficiently negatively large free-energy change for the back electron transfer ($\Delta G_{bet} = -1.5$ eV).

Fluorescence Spectra of Az−C_{60} Dyad. Figure 5a shows that S_2-S_0 fluorescence bands of Az−C_{60} dyad appeared in the 370−600 nm region upon excitation at 345 nm in toluene. Although the peak position is almost identical to that of BuAz, the intensity of the S_2-S_0 fluorescence of Az−C_{60} dyad is quite weak compared to that of BuAz by a factor of 1/5; thus, the fluorescence quantum yield of Az−C_{60} dyad was evaluated as 0.005. This finding indicates the existence of a deactivation process other than fluorescence and internal conversion. Figure 5b shows fluorescence spectra of Az−C_{60} dyad and $NMPC_{60}$ observed around 720 nm in toluene upon excitation with the 380 nm light, at which 72% of the photon is absorbed by the C_{60} moiety of the dyad. The fluorescence band from the C_{60} moiety of Az−C_{60} dyad was quenched extensively (<1/10) in a comparison with $NMPC_{60}$, the absorption intensity of which was adjusted so the same number of photons are absorbed by the C_{60} moiety at the excitation wavelength. This finding indicates that the deactivation pathway exists in the lowest singlet excited state of the C_{60} moiety such as an energy-transfer process, since the charge-separated state of Az−C_{60} dyad in toluene is expected to be at a higher energy level than Az(S_0)−C_{60}(S_1) by 0.78 eV as indicated in a schematic energy diagram calculated by the Weller equation (Figure 6a).[24] In the energy diagram, the higher excited energy levels of the C_{60} moiety have not been revealed precisely yet; thus, Az(S_0)−C_{60}(S_n) may be Az(S_0)−C_{60}(S_2) or Az(S_0)−C_{60}(S_3).

In benzonitrile, the fluorescence band from the C_{60} moiety of Az−C_{60} dyad was completely quenched. This result suggests an additional quenching process of Az(S_0)−C_{60}(S_1) in polar solvents such as a charge-separation process. In Az−C_{60} dyad, fast photoinduced intramolecular charge separation would be

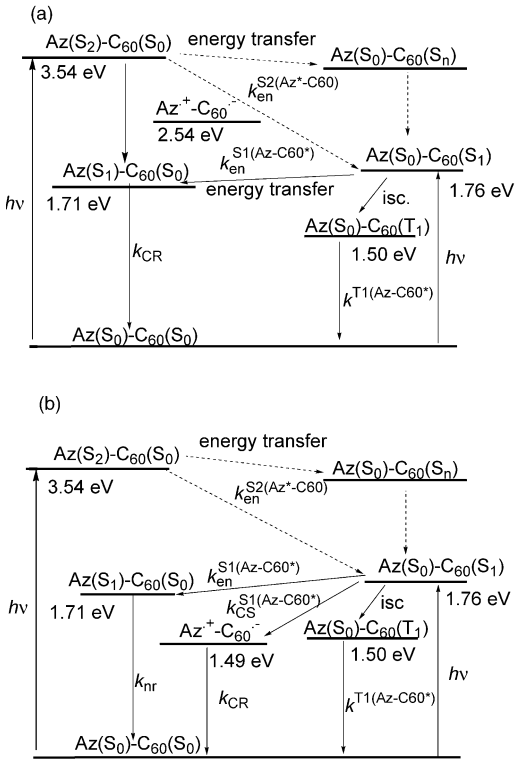

Figure 6. Schematic energy diagrams for photoinduced intramolecular processes in Az−C_{60} in (a) toluene and (b) benzonitrile. The numbers indicate energies (eV) relative to that of the ground state, and k_{nr} is rate constant for nonradiative decay. In Az(S_0)−C_{60}(S_n), *n* may be 2 or 3.

expected for the singlet excited state of the Az or C_{60} moieties, because the charge-separated state is lower than the singlet excitation energies, which makes the driving force of the electron transfer large.

Time-Resolved Fluorescence Studies. A decay profile of the S_2-S_0 fluorescence of the Az moiety of Az−C_{60} dyad at 380 nm was obtained as shown in the inset of Figure 5a. The fluorescence decay needed two exponential functions for an adequate fit, although the contribution of the long-lifetime component was quite small (<10%). The fluorescence lifetime (τ_F) of the main fast decay component of Az(S_2)−C_{60}(S_0) at 380 nm was 0.26 ns in toluene, which is far shorter than that of BuAz (1.4 ns), indicating energy transfer predominantly occurs. In benzonitrile, the τ_F value was 0.27 ns, which is almost the same as that in toluene. These results show that the quenching pathway from the S_2 state of the Az moiety in Az−C_{60} does not depend on the solvent polarity; i.e., no charge separation via the Az(S_2) moiety. Therefore, it was concluded that energy transfer from the S_2 state of the Az moiety to the C_{60} moiety generating finally Az(S_0)−C_{60}(S_1) is a main process (Figure 6), in which Az(S_0)−C_{60}(S_n) should be included as shown in the energy diagram (Figure 6, vide supra). The rate constant ($k_{en}^{S_2(Az*-C_{60})}$) for intramolecular energy transfer generating Az(S_0)−C_{60}(S_n) from Az(S_2)−C_{60}(S_0) is estimated to be 3.1×10^9 s^{-1} from eq 2, where $\tau_F^{S_2(Az*-C_{60})}$ and $\tau_F^{S_2(BuAz*)}$ are lifetimes

$$k_{en}^{S_2(Az*-C_{60})} = 1/\tau_F^{S_2(Az*-C_{60})} - 1/\tau_F^{S_2(BuAz*)} \qquad (2)$$

of the S_2-S_0 fluorescence of the Az moiety of Az−C_{60} dyad and BuAz, respectively. The $k_{en}^{S_2(Az*-C_{60})}$ value contains energy transfer to Az(S_0)−C_{60}(S_n), where *n* may be 1, 2, and 3. In our measurements employed in the presence study, the *n* value was not discriminated.

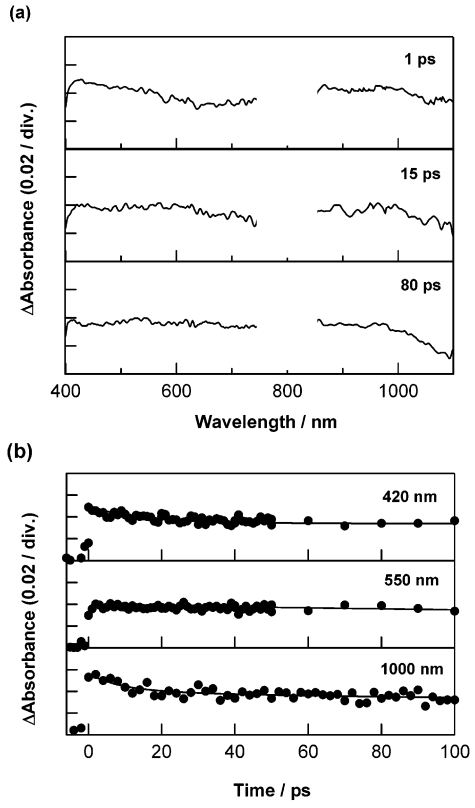

Figure 7. (a) Subpicosecond transient absorption spectra observed by 388 nm laser light excitation of Az−C_{60} (0.3 mM) in benzonitrile and (b) time profiles at 420, 550, and 1000 nm (the solid lines show the fitting curve).

As for the fluorescence from the C_{60} moiety of Az−C_{60} dyad in toluene and benzonitrile, the decay profiles were fitted to two-exponential functions (inset of Figure 5b). The τ_F values of the fast components were shorter than the present instrumental limit (<20 ps). Such short τ_F values suggest efficient intramolecular energy transfer and/or charge separation. For detailed analyses of the excited singlet processes of the C_{60} moiety, subpicosecond laser flash photolysis was carried out in the next section.

In the case of Naph−C_{60} dyad, the τ_F value of the C_{60} moiety was 1.3 ns in toluene, THF, and benzonitrile, which is the same as that of $NMPC_{60}$, indicating that no additional deactivation pathway exists in the singlet excited state of the C_{60} moiety other than the intersystem crossing to the $C_{60}(T_1)$ moiety.

Picosecond Laser Flash Photolysis. Upon excitation of Az−C_{60} dyad in benzonitrile with the femtosecond laser at 388 nm, which excited the C_{60} and Az moieties at a ratio of 72:28, transient absorption spectra were observed as shown in Figure 7a. At 1 ps an absorption band in the 420−450 nm region and a broad band in the 850−1100 nm region appeared. These absorption bands are attributed to the $S_1 \rightarrow S_n$ transition of the C_{60} moiety.[25] At 15 and 80 ps after the laser irradiation, the flat absorption in the near-IR region changes to the round absorption band characteristic of the radical anion of the $NMPC_{60}$ moiety. The small absorption band appearing in the 500−600 nm region can be attributed to the radical cation of the Az moiety. Combining these observations, generation of $Az^{\bullet+}-C_{60}^{\bullet-}$ via $Az(S_0)-C_{60}(S_1)$ can be concluded. Compared with the sharp absorption of pristine $C_{60}^{\bullet-}$ at 1080 nm in Figure 3, the absorption of the $C_{60}^{\bullet-}$ moiety of $Az^{\bullet+}-C_{60}^{\bullet-}$ at 850−1000 nm in Figure 7 was broad and weak, because the extinction coefficient of the radical anion of $NMPC_{60}$ was quite small.[26] The small quantum yield for the charge separation also makes the observation of the absorption band of the radical ions difficult (vide infra).

As shown in Figure 7b, the absorption band at 420 nm of $Az(S_0)-C_{60}(S_1)$ showed rapid decay in the initial time region until 5 ps followed by slow decay until 100 ps. The absorption−time profile at 550 nm of $Az^{\bullet+}-C_{60}^{\bullet-}$ showed a rise in the initial time region followed by slow decay until 100 ps, which continues over a few nanoseconds. At 1000 nm, the decay of $Az(S_0)-C_{60}(S_1)$ was observed. The least-squares fittings for the rising profile at 550 nm and the decaying profiles at 420 and 1000 nm in the initial time region with consideration of the rises indicate that the decay rate constant of the $Az(S_0)-C_{60}(S_1)$ state is 1.4×10^{11} s^{-1}, which is referred to as $k_{obs}^{S_1(Az-C_{60}*)}$ as listed in Table 2. Similar intramolecular charge separation was also observed in THF, and the $k_{obs}^{S_1(Az-C_{60}*)}$ value is listed in Table 2.

In the time region shorter than 1 ns, the contribution of the generation of the dissociated radical ions such as $Az^{\bullet+}-C_{60}$ and $Az-C_{60}^{\bullet-}$, which may be produced by intermolecular photoinduced electron transfer via $Az(S_0)-C_{60}(T_1)$, can be neglected, since the intermolecular process is quite slow as shown in Figure 3. Formation of $Az^{\bullet+}-C_{60}$ and $Az-C_{60}^{\bullet-}$ by disproportionation may be slower, because the bimolecular process with a diffusion-controlled limit is as slow as the time profile shown in Figure 4.

In toluene, transient spectra observed upon excitation of Az−C_{60} dyad with the femtosecond laser at 388 nm showed a flat absorption band at 1 ps in the 850−1100 nm region (inset of Figure 8), which is characteristic of the $S_1 \rightarrow S_n$ transition of the C_{60} moiety. The flat absorption does not change shape even after 50 ps. Thus, no absorption band due to the charge-separated state was confirmed. This observation is supported by the energetically inaccessible charge-separated state from $Az(S_0)-C_{60}(S_1)$ as shown in Figure 6a.

Figure 8 shows the time profile of Az−C_{60} dyad in toluene at 900 nm; it decreased quickly till 20 ps to ca. 1/3. This quick decay can be attributed to intramolecular energy transfer from the $C_{60}(S_1)$ moiety to the $Az(S_0)$ moiety in $Az(S_0)-C_{60}(S_1)$, generating $Az(S_1)-C_{60}(S_0)$. By applying the first-order decay function to the fast decay component, the decay rate constant ($k_{obs}^{S_1(Az-C_{60}*)}$) of $Az(S_0)-C_{60}(S_1)$ was estimated to be 1.2×10^{11} s^{-1} in toluene. Since the charge-separation process is not included in the deactivation process from $Az(S_0)-C_{60}(S_1)$ in toluene, the rate constant ($k^{S_1(Az-C_{60}*)}$) for the energy transfer generating $Az(S_1)-C_{60}(S_0)$ can be estimated to be 1.2×10^{11} s^{-1} from eq 3, where $k_0^{S_1(C_{60}*)}$ is referred to as the decay rate constant for the S_1 state of $NMPC_{60}$ (7.7×10^8 s^{-1}).

$$k_{en}^{S_1(Az-C_{60}*)} = k_{obs}^{S_1(Az-C_{60}*)} - k_0^{S_1(C_{60}*)} \quad (3)$$

As shown in Figure 8, the absorption of the $C_{60}(S_1)$ moiety of Az−C_{60} dyad did not decrease completely. From the slow decay of this remaining part, the decay rate constant of the slow component was 3.9×10^9 s^{-1}, which is almost the same as the fluorescence decay rate of the S_2 state of the Az moiety (3.8×10^9 s^{-1}). This finding supports that the slow decay of $Az(S_0)-C_{60}(S_1)$ is observable via slow energy transfer from $Az(S_2)-C_{60}(S_0)$, which is the rate-determining step, followed by the fast energy transfer, i.e., $Az(S_0)-C_{60}(S_1) \rightarrow Az(S_1)-C_{60}(S_0)$.

The rate constants for charge separation in the Az−C_{60} dyad ($k_{CS}^{S_1(Az-C_{60}*)}$) in polar solvents were estimated from eq 4, where

$$k_{CS}^{S_1(Az-C_{60}*)} = k_{obs}^{S_1(Az-C_{60}*)} - k_{en}^{S_1(Az-C_{60}*)} - k_0^{S_1(C_{60}*)} \quad (4)$$

TABLE 2: Free-Energy Changes for Charge Separation ($-\Delta G_{CS}^{S_1(D-C_{60}*)}$), Decay Rate Constants of the $C_{60}(S_1)$ Moiety ($k_{obs}^{S_1(D-C_{60}*)}$), Charge-Separation Rate Constants ($k_{CS}^{S_1(D-C_{60}*)}$), and Quantum Yields for Charge Separation ($\Phi_{CS}^{S_1(D-C_{60}*)}$) from the $C_{60}(S_1)$ Moieties of Az−C_{60}, Naph−C_{60}, and $NMPC_{60}$ in Various Solvents[a]

compound	solvent	ϵ_{solv}[b]	$-\Delta G_{CS}^{S_1(D-C_{60}*)}$[c]/eV	$k_{obs}^{S_1(D-C_{60}*)}$[d]/s^{-1}	$k_{CS}^{S_1(D-C_{60}*)}$[e]/s^{-1}	$\Phi_{CS}^{S_1(D-C_{60}*)}$[f]
Az−C_{60}	benzonitrile	25.2	0.27	1.4×10^{11}	0.2×10^{11}	0.14
	THF	7.58	0.04	1.3×10^{11}	0.1×10^{11}	0.07
	toluene	2.38	−0.78	1.2×10^{11}		0.00
Naph−C_{60}	benzonitrile	25.2	−0.24	7.7×10^{8}	$<10^{7}$	0.00
	THF	7.58	−0.50	7.7×10^{8}	$<10^{7}$	0.00
	toluene	2.38	−1.31	7.7×10^{8}	$<10^{7}$	0.00
$NMPC_{60}$	toluene	2.38		7.7×10^{8}		

[a] D in the superscript indicates Az or Naph. [b] Dielectric constant of the solvent. [c] $\Delta G_{CS}^{S_1(D-C_{60}*)}$ values were estimated from the Weller equation[24] by assuming that the radical radii of C_{60}, Az, and Naph moieties are 4.2, 2.6, and 2.7 Å, respectively. The center-to-center distances of Az−C_{60} and Naph−C_{60} are 8.9 and 8.5 Å, respectively, from Figure 2. The excitation energy of C_{60} is 1.76 eV. [d] From the initial decay at 900 and 420−450 nm in the picosecond transient absorption measurements. [e] $k_{CS}^{S_1(D-C_{60}*)} = k_{obs}^{S_1(D-C_{60}*)} - k_{en}^{S_1(D-C_{60}*)} - k_0^{S_1(C_{60}*)}$ (eq 4), where $k_{en}^{S_1(D-C_{60}*)}$ and $k_0^{S_1(D-C_{60}*)}$ are the energy transfer rate (1.2×10^{11} s^{-1}) and singlet decay rate of $NMPC_{60}$ (7.7×10^{8} s^{-1}), respectively. [f] $\Phi_{CS}^{S_1(D-C_{60}*)} = k_{CS}^{S_1(D-C_{60}*)}/(k_{CS}^{S_1(D-C_{60}*)} + k_{en}^{S_1(D-C_{60}*)} + k_0^{S_1(C_{60}*)})$ (eq 5).

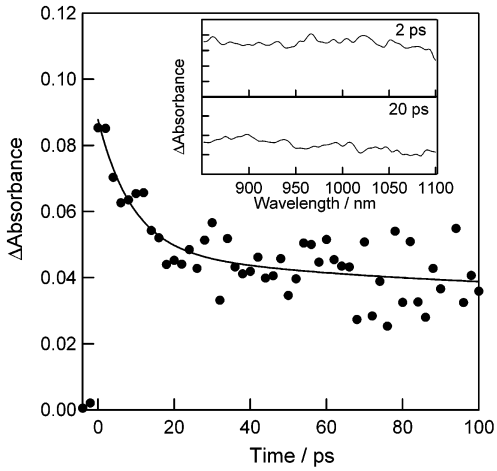

Figure 8. Time profile at 900 nm observed after 388 nm laser light excitation of Az−C_{60} (0.3 mM) in toluene (the solid line shows the fitting curve). Inset: subpicosecond transient absorption spectra.

the $k_{en}^{S_1(Az-C_{60}*)}$ value in benzonitrile and THF is assumed to be equal to that in toluene (1.2×10^{11} s^{-1}), since the energy-transfer rate constant usually does not depend on the solvent polarity. The $k_{CS}^{S_1(Az-C_{60}*)}$ values in benzonitrile and THF are summarized in Table 2. The $k_{CS}^{S_1(Az-C_{60}*)}$ values in benzonitrile and THF are on the order of 10^{10} s^{-1}, which is 1 order smaller than the $k_{en}^{S_1(Az-C_{60}*)}$ value. Furthermore, the quantum yields ($\Phi_{CS}^{S_1(Az-C_{60}*)}$) for charge separation from the Az(S_0)−C_{60}(S_1) state were estimated from eq 5.

$$\Phi_{CS}^{S_1(Az-C_{60}*)} = k_{CS}^{S_1(Az-C_{60}*)}/(k_{CS}^{S_1(Az-C_{60}*)} + k_{en}^{S_1(Az-C_{60}*)} + k_0^{S_1(C_{60}*)}) \quad (5)$$

As summarized in Table 2, the $\Phi_{CS}^{S_1(Az-C_{60}*)}$ values were estimated to be 0.14 and 0.07 in benzonitrile and THF, respectively. These small $\Phi_{CS}^{S_1(Az-C_{60}*)}$ values can be attributed to small $k_{CS}^{S_1(Az-C_{60}*)}$ values compared to the $k_{en}^{S_1(Az-C_{60}*)}$ value, because the free-energy changes for charge separation ($-\Delta G_{CS}^{S_1(Az-C_{60}*)}$) are as small as 0.27 and 0.04 eV in benzonitrile and THF, respectively. The smaller rate constants and yields for charge separation are consistent with smaller absorption intensity of the radical ion species in the transient absorption spectra. Since the reorganization energies of most of the dyads including the C_{60} moiety are reported to be 0.6−0.8 eV in polar solvents,[4] the charge-separation processes of Az−C_{60} in these solvents are in the "normal region" apart from the top of the Marcus parabola.[27] This consideration is supported by the fact that the $k_{CS}^{S_1(Az-C_{60}*)}$ value in benzonitrile with negative $\Delta G_{CS}^{S_1(Az-C_{60}*)}$ is larger than that in THF with almost zero $\Delta G_{CS}^{S_1(Az-C_{60}*)}$.

As for the charge separation from the S_2 state of the Az moiety for the Az−C_{60} dyad, $-\Delta G_{CS}^{S_2(Az*-C_{60})}$ values are evaluated to be as large as 1.02−1.26 eV in polar solvents. These large $-\Delta G_{CS}^{S_2(Az*-C_{60})}$ values indicate that the charge-separation process from the S_2 state is in the Marcus "inverted region" apart from the top region of the parabola.[27] Thus, the charge-separation process is also not the major process in the S_2 state of the Az moiety, for which only smaller $k_{CS}^{S_2(Az*-C_{60})}$ than that of the competitive energy-transfer process was expected.

The contribution of the S_1 state of the Az moiety of Az−C_{60} dyad to the charge separation is also considered to be small, since the $-\Delta G_{CS}^{S_1(Az*-C_{60})}$ value is small. Furthermore, existence of the fast internal conversion from the S_1 state to the S_0 state of the Az moiety (<1 ps) makes the charge separation a minor process via Az(S_1)−C_{60}(S_0).[12]

The absorption bands due to the radical anion of the C_{60} moiety of Az−C_{60} dyad showed the decay over several nanoseconds in benzonitrile and THF. The decay can be attributed to the charge-recombination process. The rate constants for the charge recombination (k_{CR}) were estimated to be 1.0×10^{9} and 0.2×10^{9} s^{-1} in benzonitrile and THF, respectively, by curve fitting of the decay component of the C_{60} radical anion in the long time measurements; these k_{CR} values correspond to lifetimes of 1 and 5 ns, respectively. Free-energy changes for charge recombination (ΔG_{CR}) generating the ground state are summarized in Table 3. From these ΔG_{CR} values, the charge-recombination processes are expected in the Marcus inverted region.[27] This consideration is supported by the fact that the k_{CR} value in benzonitrile is larger than that in THF.

Nanosecond Laser Flash Photolysis. As described above, photoinduced charge separation via Az(S_0)−C_{60}(S_1) and the decay of $Az^{\bullet+}$−$C_{60}^{\bullet-}$ were observed by the picosecond laser flash photolysis in benzonitrile and THF; however, in the nanosecond laser flash photolysis using the 532 nm laser pulse, only the transient absorption band at 720 nm of the Az(S_0)−C_{60}(T_1) state was observed without any absorption band attributable to the charge-separated state as shown in Figure 9. This finding indicates that the lifetimes of $Az^{\bullet+}$−$C_{60}^{\bullet-}$ produced via Az(S_0)−C_{60}(S_1) were less than the pulse duration of the nanosecond laser (ca. 6 ns) even in polar solvents. This finding also excludes the photoinduced charge separation via the Az(S_0)−C_{60}(T_1) state. The decay rate constant of Az(S_0)−C_{60}(T_1), which is referred to as $k^{T_1(Az-C_{60}*)}$, was estimated to be 5.1×10^{4} s^{-1}, which is close to the value of $NMPC_{60}$(T_1);

TABLE 3: Free-Energy Changes ($-\Delta G_{CR}$), Rate Constants (k_{CR}) for Charge Recombination, Triplet Decay Rate Constants (k_T), and Quantum Yields for Triplet Formation (Φ_T) of Az−C_{60}, Naph−C_{60}, and $NMPC_{60}$ in Various Solvents

compound	solvent	$-\Delta G_{CR}$[a]/eV	k_{CR}[b]/s^{-1}	$k^{T_1(D-C_{60}*)}$[c]/s^{-1}	$\Phi^{T_1(D-C_{60}*)}$[c]
Az−C_{60}	benzonitrile	1.49	1.0×10^9	5.1×10^4	0.048
	THF	1.72	0.2×10^9	5.7×10^4	0.047
	toluene	2.54		6.1×10^4	0.051
Naph−C_{60}	benzonitrile	2.00		5.2×10^4	0.92
	THF	2.26		6.0×10^4	0.91
	toluene	3.07		4.3×10^4	0.94
$NMPC_{60}$	toluene			4.1×10^4	0.95

[a] ΔG_{CR} values were estimated assuming parameters listed in the caption of Tables 1 and 2. [b] From the decay time profiles at 1000 nm in the 20−3000 ps time region. [c] From nanosecond transient absorption measurements.

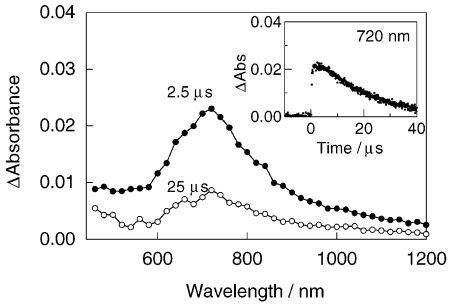

Figure 9. Nanosecond transient absorption spectra observed by 355 nm laser light excitation of Az−C_{60} (0.1 mM) in deaerated benzonitrile. Inset: absorption−time profile at 720 nm.

$k^{T_1(C_{60}*)} = 4.1 \times 10^4\ s^{-1}$. Thus, the lifetime of Az(S_0)−C_{60}(T_1) was ca. 20 μs. This finding indicates that the generated Az(S_0)−C_{60}(T_1) deactivates to the ground state by intersystem crossing without further reaction pathways even in the polar solvent as indicated in the energy diagram (Figure 6b). Similar spectra and time profiles were observed in THF and toluene.

As shown in Table 3, the quantum yields for the Az(S_0)−C_{60}(T_1) formation ($\Phi^{T_1(Az-C_{60}*)}$) were estimated to be 0.048, 0.047, and 0.051 in benzonitrile, THF, and toluene, respectively, by relative actinometry using C_{70}(T_1) as an internal standard (T−T peak at 980 nm, $\epsilon = 6500\ M^{-1}\ s^{-1}$, and $\Phi_{isc} = 0.9 \pm 0.15$).[28] These quite small $\Phi^{T_1(Az-C_{60}*)}$ values indicate that most parts of the Az(S_0)−C_{60}(S_1) state transfer its excited energy to the S_1 state of the Az moiety, producing Az(S_1)−C_{60}(S_0), which is a more efficient process than the intersystem crossing process to Az(S_0)−C_{60}(T_1). Furthermore, the $Az^{\bullet+}-C_{60}^{\bullet-}$ state deactivates to the ground state (Az(S_0)−C_{60}(S_0)) predominantly without generating the Az(S_0)−C_{60}(T_1) state. These findings indicate that the Az(S_0)−C_{60}(T_1) state was mainly generated by the intersystem crossing from the Az(S_0)−C_{60}(S_1) state because the $\Phi^{T_1(Az-C_{60}*)}$ values did not depend on the polarity of the solvents.

Naph−C_{60} dyad also showed the transient absorption band at 720 nm due to the triplet excited state of the C_{60} moiety upon excitation in benzonitrile. The decay rate constant was estimated to be $5.2 \times 10^4\ s^{-1}$, which is close to those of Az−C_{60} dyad and $NMPC_{60}$, indicating the absence of further photoinduced processes from the triplet excited state (Naph(S_0)−C_{60}(T_1)). The intensity of the transient absorption band of Naph(S_0)−C_{60}(T_1) was quite larger than that of Az(S_0)−C_{60}(T_1). The $\Phi^{T_1(Naph-C_{60}*)}$ value was estimated to be 0.92 in benzonitrile, which is close to that of $NMPC_{60}$.[26] This finding supports the consideration that the Naph(S_0)−C_{60}(S_1) state generates the Naph(S_0)−C_{60}(T_1) state almost quantitatively via the intersystem crossing, indicating the absence of the charge separation. These findings show that the donor ability of naphthalene is quite weak compared to that of azulene. The absence of energy transfer from Naph(S_0)−C_{60}(T_1) to Naph(T_1)−C_{60}(S_0) was also confirmed by such a large $\Phi^{T_1(Naph-C_{60}*)}$ value, which is reasonable because the energy level of C_{60}(T_1) is lower than that of Naph(T_1).

Conclusion

In the present study, the favorable donor ability of azulene was confirmed in the comparison with naphthalene both in the mixture systems and in the dyad molecules, even though both azulene and naphthalene have the same 10-π-electron systems. In the mixture system, intermolecular electron transfer takes place via C_{60}(T_1), while intramolecular charge separation for the Az−C_{60} dyad takes place via Az(S_0)−C_{60}(S_1) in polar solvents. Furthermore, in the Az−C_{60} dyad, two successive energy-transfer processes were confirmed, i.e., Az(S_2)−C_{60}(S_0) → Az(S_0)−C_{60}(S_n) and Az(S_0)−C_{60}(S_1) → Az(S_1)−C_{60}(S_0), in which the C_{60} moiety acts as an energy reflector from the S_2 state to the S_1 state of the Az moiety.

Acknowledgment. The present work was partly supported by a Grant-in-Aid on Scientific Research from the Japan Society for the Promotion of Science and the Ministry of Education, Science, Sports and Culture of Japan. We are also grateful for financial support by Core Research for Evolutional Science and Technology (CREST) of the Japan Science and Technology Corp. and The Mitsubishi Foundation.

References and Notes

(1) For a review, see: Wasielewski, M. *Chem. Rev.* **1992**, *92*, 435.

(2) (a) Williams, R. M.; Zwier, J. M.; Verhoeven, J. W. *J. Am. Chem. Soc.* **1995**, *117*, 4093. (b) Williams, R. M.; Koeberg, M.; Lawson, J. M.; An, Y.-Z.; Rubin, Y.; Paddon-Row: M. N.; Verhoeven, J. W. *J. Org. Chem.* **1996**, *61*, 5055. (c) Komamine, S.; Fujitsuka, M.; Ito, O.; Moriwaki, K.; Miyata, T.; Ohno, T. *J. Phys. Chem. A* **2000**, *104*, 11497.

(3) Imahori, H.; Cardoso, S.; Tatman, D.; Lin, S.; Noss, L.; Seely, G. R.; Sereno, L.; Silber, C.; Moore, T. A.; Moore, A. L.; Gust, D. *Photochem. Photobiol.* **1995**, *62*, 1009.

(4) (a) Kuciauskas, D.; Lin, S.; Seely, G. R.; Moore, A. L.; Moore, T. A.; Gust, D.; Drovetskaya, T.; Reed, C. A.; Boyd, P. D. W. *J. Phys. Chem.* **1996**, *100*, 15926. (b) Imahori, H.; Hagiwara, K.; Aoki, M.; Akiyama, T.; Taniguchi, S.; Okada, T.; Shirakawa, M.; Sakata, Y. *J. Am. Chem. Soc.* **1996**, *118*, 11771. (c) Imahori, H.; Hagiwara, K.; Akiyama, T.; Aoki, M.; Taniguchi, S.; Okada, T.; Shirakawa, M.; Sakata, Y. *Chem. Phys. Lett.* **1996**, *263*, 545. (d) Imahori, H.; Ozawa, S.; Uchida, K.; Takahashi, M.; Azuma, T.; Ajavakom, A.; Akiyama, T.; Hasegawa, M.; Taniguchi, S.; Okada, T.; Sakata, Y. *Bull. Chem. Soc. Jpn.* **1999**, *72*, 485. (e) Tkachenko, N. V.; Rantala, L.; Tauber, A. Y.; Helaja, J.; Hynninen, P. V.; Lemmetyinen, H. *J. Am. Chem. Soc.* **1999**, *121*, 9378. (f) Schuster, D. I.; Cheng, P.; Wilson, S. R.; Prokhorenko, V.; Katterle, M.; Holzwarth, A. R.; Braslavsky, S. E.; Klihm, G.; Williams, R. M.; Luo, C. *J. Am. Chem. Soc.* **1999**, *121*, 11599. (g) Fujitsuka, M.; Ito, O.; Imahori, H.; Yamada, K.; Yamada, H.; Sakata, Y. *Chem. Lett.* **1999**, 721. (h) Imahori, H.; Tamaki, K.; Guldi, D. M.; Luo, C.; Fujitsuka, M.; Ito, O.; Sakata, Y.; Fukuzumi, S. *J. Am. Chem. Soc.* **2001**, *123*, 2607. (i) Imahori, H.; Guldi, D. M.; Tamaki, K.; Yoshida, Y.; Luo, C.; Sakata, Y.; Fukuzumi, S. *J. Am. Chem. Soc.* **2001**, *123*, 2607.

(5) (a) Llacay, J.; Veciana, J.; Vidal-Gancedo, J.; Bourdelnde, J. L.; González-Moreno, R.; Rovira, C. *J. Org. Chem.* **1998**, *63*, 5201. (b) Martin, N.; Sánchez, L.; Herranz, M. A.; Guldi, D. M. *J. Phys. Chem. A* **2000**, *104*, 4648.

(6) (a) Yamashiro, T.; Aso, Y.; Otsubo, T.; Tang, H.; Harima, T.; Yamashita, K. *Chem. Lett.* **1999**, 443. (b) Fujitsuka, M.; Ito, O.; Yamashiro,

T.; Aso, Y.; Otsubo, T. *J. Phys. Chem. A* **2000**, *104*, 4876. (c) Fujitsuka, M.; Matsumoto, K.; Ito, O.; Yamashiro, T.; Aso, Y.; Otsubo, T. *Res. Chem. Intermed.* **2001**, *27*, 73. (d) Hirayama, D.; Yamashiro, T.; Takimiya, K.; Aso, Y.; Otsubo, T.; Norieda, H.; Imahori, H.; Sakata, Y. *Chem. Lett.* **2000**, 570. (e) van Hal, P. A.; Knol, J.; Longeveld-Voss, B. M. W.; Meskers, S. C. J.; Hummelen, J. C.; Janssen, R. A. J. *J. Phys. Chem. A* **2000**, *104*, 5974. (f) Fujitsuka, M.; Masuhara, A.; Kasai, H.; Oikawa, H.; Nakanishi, H.; Ito, O.; Yamashiro, T.; Aso, Y.; Otsubo, T. *J. Phys. Chem. B* **2001**, *104*, 9930.

(7) (a) Sariciftci, N. S.; Wudl, F.; Heeger, A. J.; Maggini, M.; Scorrano, G.; Prato, M.; Bourassa, J.; Ford, P. C. *Chem. Phys. Lett.* **1995**, *247*, 510. (b) Maggini, M.; Guldi, D. M.; Mondini, S.; Scorrano, G.; Paolucci, F.; Ceroni, P.; Roffia, S. *Chem.—Eur. J.* **1998**, *4*, 1992. (c) Polese, A.; Mondini, S.; Bianco, A.; Toniolo, C.; Scorrano, G.; Guldi, D. M.; Maggini, M. *J. Am. Chem. Soc.* **1999**, *121*, 3446. (d) Guldi, D. M.; Garscia, G. T.; Mattay, J. *J. Phys. Chem. A* **1998**, *102*, 9679. (e) Guldi, D. M. *Chem. Commun.* **2000**, 321. (f) Yamazaki, M.; Araki, Y.; Fujitsuka, M.; Ito, O. *J. Phys. Chem. A* **2001**, *105*, 8615. (g) Guldi, D. M.; Swartz, A. S.; Luo, C.; Gómez, R.; Segura, J. L.; Martín, N. *J. Am. Chem. Soc.* **2002**, *124*, 10875. (h) Fujitsuka, M.; Luo, H.; Murata, Y.; Kato, N.; Ito, O.; Komatsu, K. *Chem. Lett.* **2002**, 968.

(8) (a) Prato, M.; Maggini, M.; Giacometti, C.; Scorrano, G.; Sandonà, G.; Farnia, G. *Tetrahedron* **1996**, *52*, 5221. (b) Guldi, D. M.; Maggini, M.; Scorrano, G.; Prato, M. *J. Am. Chem. Soc.* **1997**, *119*, 974.

(9) (a) D'Souza, F.; Zandler, M. E.; Smith, P. M.; Deviprasad, G. R.; Arkady, K.; Fujitsuka, M.; Ito, O. *J. Phys. Chem. A* **2002**, *106*, 649. (b) D'Souza, F.; Zandler, M. E.; Smith, P. M.; Deviprasad, G. R.; Arkady, K.; Fujitsuka, M.; Ito, O. *J. Org. Chem.* **2002**, *67*, 9122.

(10) (a) Peeters, E.; van Hal, P. A.; Knol, J.; Brabec, C. J.; Saricifitci, N. S.; Hummelen, J. C.; Janssen, R. A. J. *J. Phys. Chem. B* **2000**, *104*, 10174. (b) Apperloo, J. J.; Martineau, C.; van Hal, P. A.; Roncali, J.; Janssen, R. A. J. *J. Phys. Chem. A* **2002**, *106*, 21.

(11) (a) Kasha, M. *Discuss. Faraday Soc.* **1950**, *9*, 14. (b) Binsch, G.; Heilbronner, E.; Jankow, R.; Schmidt, D. *Chem. Phys. Lett.* **1967**, *1*, 135. (c) Murata, S.; Iwanaga, C.; Toda, T.; Kokubun, H. *Ber. Bunsen-Ges. Phys. Chem.* **1972**, *76*, 1176.

(12) (a) Gillespie, G. D.; Wild, U. P. *Chem. Phys.* **1980**, *52*, 117. (b) Rentzepis, P. M. *Chem. Phys. Lett.* **1968**, *2*, 117. (c) Wagner, B. D.; Helmrich, D. T.; Steer, R. P. *J. Phys. Chem.* **1992**, *96*, 7904. (d) Wagner, B. D.; Szymanski, M.; Steer, R. P. *J. Chem. Phys.* **1993**, *98*, 301. (e) Abou-Zied, O. K.; Sinha, H. K.; Steer, R. P. *J. Phys. Chem. A* **1997**, *101*, 7989. (f) Tétreault, N.; Muthyala, R. S.; Liu, R. S. H.; Steer, R. P. *J. Phys. Chem. A* **1999**, *103*, 2524.

(13) (c) Yeow, E. K.; Steer, R. P. *Phys. Chem. Chem. Phys.* **2003**, *5*, 97.

(14) Ito, S.; Morita, N.; Asao, T. *Bull. Chem. Soc. Jpn.* **1995**, *68*, 1409.

(15) Maggini, M.; Scorrano, G.; Prato, M. *J. Am. Chem. Soc.* **1993**, *115*, 9798.

(16) Guldi, D. M.; Luo, C.; Swartz, A.; Gómez, R.; Segura, J. L.; Martín, N.; Brabec, C.; Sariciftci, N. S. *J. Org. Chem.* **2002**, *67*, 1141.

(17) Frisch, M. J.; Trucks, G. W.; Schlegel, H. B.; Scuseria, G. E.; Robb, M. A.; Cheeseman, J. R.; Zakrzewski, V. G.; Montgomery, J. A., Jr.; Stratmann, R. E.; Burant, J. C.; Dapprich, S.; Millam, J. M.; Daniels, A. D.; Kudin, K. N.; Strain, M. C.; Farkas, O.; Tomasi, J.; Barone, V.; Cossi, M.; Cammi, R.; Mennucci, B.; Pomelli, C.; Adamo, C.; Clifford, S.; Ochterski, J.; Petersson, G. A.; Ayala, P. Y.; Cui, Q.; Morokuma, K.; Rega, N.; Salvador, P.; Dannenberg, J. J.; Malick, D. K.; Rabuck, A. D.; Raghavachari, K.; Foresman, J. B.; Cioslowski, J.; Ortiz, J. V.; Baboul, A. G.; Stefanov, B. B.; Liu, G.; Liashenko, A.; Piskorz, P.; Komaromi, I.; Gomperts, R.; Martin, R. L.; Fox, D. J.; Keith, T.; Al-Laham, M. A.; Peng, C. Y.; Nanayakkara, A.; Challacombe, M.; Gill, P. M. W.; Johnson, B.; Chen, W.; Wong, M. W.; Andres, J. L.; Gonzalez, C.; Head-Gordon, M.; Replogle, E. S.; Pople, J. A. *Gaussian 98*, Revision A.11.3; Gaussian, Inc.: Pittsburgh, PA, 2002.

(18) Shida, T. *Electronic Absorption Spectra of Radical Ions*; Elsevier: Amsterdam, 1988.

(19) Plattner, P. A.; Heilbronner; E.; Weber, S. *Helv. Chim. Acta* **1952**, *35*, 1036.

(20) (a) Biczok, L.; Linshitz, H.; Walter, R. I. *Chem. Phys. Lett.* **1992**, *195*, 339. (b) Fujitsuka, M.; Luo, C.; Ito, O. *J. Phys. Chem. B* **1999**, *103*, 445.

(21) (a) Steren, C. A.; van Willigen, H.; Biczok, L.; Gupta, N.; Linschitz, H. *J. Phys. Chem.* **1996**, *100*, 8920. (b) Alam, M. M.; Watanabe, A.; Ito, O. *J. Photochem. Photobiol., A* **1997**, *104*, 59.

(22) Murov, S. L.; Carmichael, I.; Hug, G. L. *Handbook of Photochemistry*, 2nd ed.; Marcel Dekker: New York, 1993.

(23) Rehm, D.; Weller, A. *Isr. J. Chem.* **1970**, *8*, 259.

(24) Weller, A. *Z. Phys. Chem.* **1982**, *133*, 93.

(25) (a) Ebbesen, T. W.; Tanigaki, K.; Kuroshima, S. *Chem. Phys. Lett.* **1991**, *181*, 501. (b) Watanabe, A.; Ito, O.; Watanabe, M.; Saito, H.; Koishi, M. *J. Chem. Soc., Chem. Commun.* **1996**, 117.

(26) Luo, C.; Fujitsuka, M.; Watanabe, A.; Ito, O.; Gan, L.; Huang, Y. Huang, C.-H. *J. Chem. Soc., Faraday Trans.* **1998**, *94*, 527.

(27) (a) Marcus, R. A. *Annu. Rev. Phys. Chem.* **1964**, *15*, 144. (b) Marcus, R. A.; Sutin, N. *Biochim. Biophys. Acta* **1985**, *811*, 265. (c) Marcus, R. A. *Angew. Chem., Int. Ed. Engl.* **1993**, *32*, 1111.

(28) (a) Guldi, D. M.; Hungerbuhler, H.; Janata, E.; Asmus, K.-D. *J. Phys. Chem.* **1993**, *97*, 11258. (b) Fraelich, M. R.; Weisman, R. B. *J. Phys. Chem.* **1993**, 97, 11145. (c) Alam, M. M.; Watanabe, A.; Ito, O. *Bull. Chem. Soc. Jpn.* **1997**, *70*, 1833.